Radiolabeling of Nanoshells with ^{64}Cu and ^{111}In for PET and SPECT Imaging in Rats

Huan Xie[1*], Zheng Jim Wang[2,3], Ande Bao[2], Beth Goins[2], William T. Phillips[2], Chris L. Coleman[4]

[1*] Department of Pharmaceutical Sciences, College of Pharmacy and Health Sciences, Texas Southern University, Houston, Texas, xieh@tsu.edu; [2]Department of Radiology, University of Texas Health Science Center at San Antonio, San Antonio, Texas; [3]MPI Research, Inc., Mattawan, MI; [4]Nanospectra Biosciences, Inc., Houston, Texas

ABSTRACT

Here we report for the first time the radioactive labeling of gold nanoshells with ^{64}Cu and ^{111}In. A conjugation method was developed to link nanoshells with the radioactive tags. The resulting conjugates showed good labeling efficiency and stability in PBS and serum for *in vivo* imaging applications. The circulation of ^{64}Cu-nanoshells and ^{111}In-nanoshells in mice were determined by dynamic light scattering and their blood clearance in rats were determined in terms of radioactive counting. By PET/CT and SPECT/CT imaging, we monitored the *in vivo* distribution of ^{64}Cu-nanoshells and ^{111}In-nanoshells in nude rats with a head and neck squamous cell carcinoma xenograft at various time points after their intravenous injection. PET and SPECT images of the rats showed that both of the labeled nanoshells accumulated in the tumor. PET images with ^{64}Cu showed better resolution and were therefore, more promising for future applications.

Keywords: nanoshells, radiolabeling, PET, SPECT, cancer

1 INTRODUCTION

Nanostructures have been intensively studied and broadly utilized for biological applications, such as molecular imaging, molecular diagnosis and targeted therapy. Among these new nanostructures, nanoshells are of special interest for cancer treatment because of their unique size, composition, physical and optical properties. Nanoshells are spherical nanoparticles consisting of a dielectric core and a metal shell, where the plasmon resonance frequency is determined by the relative size of the core and the metal shell layer [1]. By adjusting the relative core and shell thicknesses, nanoshells can be fabricated that will absorb or scatter light across the visible and near-infrared regions (NIR) of the electromagnetic spectrum. Silica core gold nanoshells were made by biocompatible materials, and the surface was modified with "stealthing" polymers like polyethylene glycol (PEG) to further improve the biocompatibility [2]. They were manufactured with size ranges that can accumulate in tumors via the enhanced permeability and retention (EPR) effect. Nanoshell-based photo-thermal ablation has been demonstrated to be effective in the elimination of solid tumors in animal models [2, 3].

The fate and biological effects of nanoshells in animals are critical to their applications *in vivo*. However, we have not seen any prior reports on the biodistribution of nanoshells. The *in vivo* biodistributions of some popular nanoparticles have been reported, such as carbon nanotubes and quantum dots (QDs). The biodistribution and tumor targeting ability of radio-labeled carbon nanotubes has been investigated in rats and mice by *in vivo* positron emission tomography (PET) and single photon emission computed tomography (SPECT) [4, 5]. Cai *et al.* reported the *in vivo* targeting and imaging of tumor vasculature using RGD peptide-QD conjugates [6].

In this paper we report the procedure of labeling gold nanoshells with the radionuclide labels, copper-64 (^{64}Cu) and indium-111 (^{111}In), and the biodistribution of the radiolabeled nanoshells in live rats by positron emission tomography (PET) and single-photon emission computed tomography (SPECT) imaging. Classical biodistribution studies that quantify radiolabeled particles deposition provide results in terms of populational averages at specific time points, but do not allow particle localization to be tracked longitudinally in individual animals. PET and SPECT are noninvasive imaging tools that allow researchers to quantitatively image the uptake of candidate nanoparticles at the target site with high sensitivity in real time. In addition to conventional ex vivo biodistribution techniques, the pharmacokinetic profile of new nanomaterials with potential medical applications can be obtained with PET and SPECT studies on a relatively small number of laboratory animals [7].

2 MATERIALS AND METHODS

2.1 Radiolabeling of NS and Stability Test

Gold-Silica nanoshells (NS) were synthesized as previously described [8]. NS formation was assessed using a UV-VIS spectrophotometer (U-0080D, Hitachi) and Zetasizer (Nano-ZS, Malvern). NS manufactured in this manner have a 8-10 nm gold shell around a 110-120 nm silica sphere.

The labeling process is shown in Figure 1. First, a bi-functional chelating agent p-NH2-Bn-DOTA (S-2-(4-

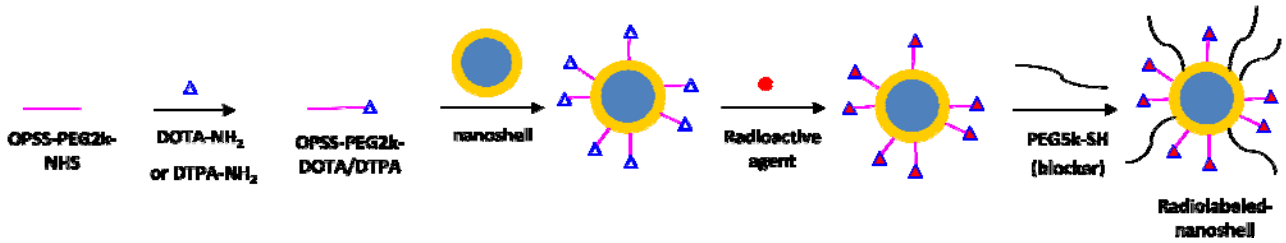

Figure 1: The cartoon scheme of labeling a radioactive agent to NS.

Aminobenzyl)-1,4,7,10-tetraazacyclododecane tetraacetic acid, for ^{64}Cu labeling) or p-NH2-Bn-DTPA (S-2(4-Aminobenzyl)-diethylenetriamine pentaacetic acid, for ^{111}In labeling) (Macrocyclics) was conjugated to another bi-functional OPSS-PEG2k-NHS (opyridyldisulfide-polyethylene glycol 2000- N-hydroxysuccinimide ester) (Nektar). DOTA (or DTPA) and PEG2k were mixed with 1:1 molar ratio for overnight at RT. The resulting OPSS-PEG-DOTA (or OPSS-PEG-DTPA) was then added to NS solution (in 10 mM phosphate buffer, pH7) with 10,000:1 molar ratio for overnight at RT on a shaker, allowing the OPSS group to conjugate to the gold surface of the particles. The mixture was centrifuged and the supernatant with unconjugated OPSS-PEG-DOTA or OPSS-PEG-DTPA was removed. The pellets of DOTA-NS and DTPA-NS were re-suspended in phosphate buffer and checked with spectrophotometer and Zetasizer to determine the NS concentration and size for further conjugation.

All the radioactive research was performed at Department of Radiology, UTHSC-San Antonio. $^{64}CuCl_2$ (Washington University, St. Louis, MO) was diluted in 30 mM ammonia citrate buffer (pH 6.5). Then 816 µCi of ^{64}Cu was added to 150 µL of the DOTA-NS solution (~0.8 nM) prepared above and incubated at 37 ^{o}C for 90 min. Then blocking agent PEG5k-SH (Nektar) was added to NS solution with 300,000:1 molar ratio and incubated at RT on a shaker for 1 hr. The mixtures were then centrifuged to remove unconjugated ^{64}Cu and PEG5k. Labeling of $^{111}InCl_3$ (GE Healthcare, San Antonio, TX) was following the same procedure. The supernatants and pellets were collected for radioactive counting. Labeling efficiencies were calculated by using the relation: [activity in pellet/(activity in supernatant + activity in pellet)] x 100.

The stability tests were investigated by incubating ^{64}Cu-NS and ^{111}In-NS in PBS and serum at 37 ^{o}C for up to 20 hr. Suspensions were divided to several equal parts and at each time point one was taken for centrifugation. The supernatants and pellets were collected for radioactive counting. Percentages of ^{64}Cu and ^{111}In remaining on the NS were calculated by using the relation: [activity in pellet/(activity in supernatant + activity in pellet)] x 100.

2.2 Estimation of NS Circulation *in vivo* Using Dynamic Light Scattering.

Animal studies performed at Nanospectra Biosciences, Inc. were under the guidelines of the Guide for the Care and Use for Laboratory Animals and was approved by the Institutional Animal Care and Use Committee. Female mice (5-8 weeks age, 14-20g, Harlan) were anesthetized with Avertin (20 µL/g, 1.2% solution, VWR), and then intravenously injected with 8 µL/g (NS volume/mouse body weight) of normal NS to one mouse and DOTA-NS to two mice (~1 X 10^{11} NS per mL). Allowing for rapid particle dispersal in the murine vascular system, a series of 10.5 – 15 µL blood samples were collected, starting at approximately 15 minutes after the injection. Those blood samples were prepared for analysis by dilution with a 5% (v/v) Triton X-100 aqueous solution (VWR), resulting in a 3% (v/v) blood solution [9]. After a 5 minute incubation period for cell lysis, three repeated DLS measurements (Nano-ZS, Malvern) were collected using the "general purpose mode" algorithm (≈ 2 min for each measurement).

2.3 Intravenous Injection, Imaging and Blood Sample Collection.

A human head and neck squamous cell carcinoma (HNSCC) xenograft model in nude rats was established via subcutaneous inoculation of a HNSCC cell line, SCC-4 [10]. Animal experiments with radioactive agents were done at UTHSC according to the NIH Animal Use guidelines. On the day of imaging, the average tumor volume for the ^{64}Cu-NS group (n=4) and ^{111}In-NS group (n=4) were 1.2 cm^3 and 1.0 cm^3, respectively. During all procedures, the nude rats (~150 g) were anesthetized with Avertin (400 mg/kg) by IP injections. ^{64}Cu-NS or ^{111}In-NS were injected manually into the rats' tail vein at about 0.5 ml per minute. PET and SPECT imaging was performed at 1 hr, 4hr, 20hr and 44hr post injection of radiolabeled NS with the FLEX X-PET/CT/SPECT (Gamma Medica-Ideas, Inc., Northridge, CA) followed by CT image acquisition.

Blood samples (40 µL) were collected from the opposite tail vein from the injection at 5 min, 1 hr, 4 hr, 20 hr, and 44 hr time points after intravenous injection. The ^{64}Cu and ^{111}In radioactivity in blood samples were measured by a γ-counter. The values of blood circulation half-life were obtained by second-order exponential decay fitting.

3 RESULTS AND DISCUSSION

Nanoshells used in this study were manufactured to be comprised of a silica core (~120 nm in diameter) and a gold

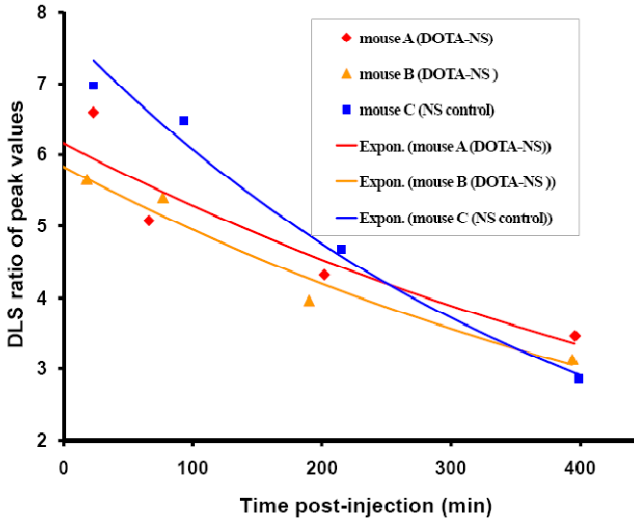

Figure 2: Mice circulation curves of DOTA-NS versus normal NS determined by DLS peak ratios.

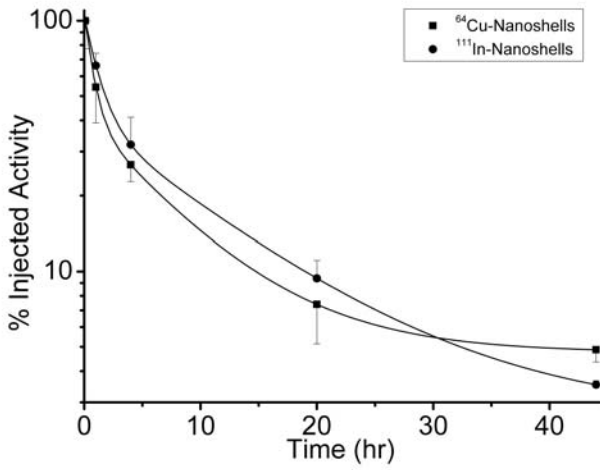

Figure 3: The blood clearance of ^{64}Cu-NS and ^{111}In-NS in rats determined by radioactive counting

shell (8~10 nm) to absorb light at the near infrared region. The UV-VIS spectrum showed the NS peak at ~760 nm. Zetasizer measurements showed the NS size is around 140 nm in diameter and zeta potential is around -50V. Those data met our criteria for normal NS batch manufacture.

A conjugation procedure was developed to label NS with ^{64}Cu, $t_{1/2}$ =12.7hr and ^{111}In, $t_{1/2}$ = 2.8 days using bifunctional OPSS-PEG2K-NHS and bifunctional chelating agent DOTA-NH_2 or DTPA-NH_2 (Figure 1). First, OPSS-PEG2K-NHS and DOTA-NH_2 or DTPA-NH_2 were mixed, and the NHS ester reacted with the amine group to form an amide bond. The mixture was then added to an NS solution allowing the OPSS group to attach to the gold surface of the particles. NS were then incubated with $^{64}CuCl_2$ or $^{111}InCl_3$. Finally the longer PEG5K-thiol was added to block the remaining empty areas on the gold surface to provide better PEG coverage.

The radioactively labeled particles were thoroughly washed twice by centrifugation and re-suspension in fresh PBS buffer. The radioactive signal from both the pellet and the supernatant was measured in the dose calibrator to obtain the labeling efficiency, which is the radioactive count in the pellet vs. the total radioactive count. The average radiolabeling efficiency (n=3) was 81.3% and 80.32% for ^{64}Cu-NS and ^{111}In-NS respectively after 2 separations.

Prior to any *in vivo* examination of ^{64}Cu-NS and ^{111}In-NS, *in vitro* stabilities in PBS and serum were tested. The labeled particles were incubated with either serum or PBS (control) for 1hr, 3 hr and 18 hr. At each time point, samples were centrifuged and the supernatant removed. The radioisotope content of both the pellet and supernatant was determined by dose calibrator. The percentage of ^{64}Cu remaining on the particles after 18 hr incubation with PBS and serum were 87% and 45% respectively. The percentage of ^{111}In remaining on the particles after 19 hr incubation with PBS and serum were 95% and 45% respectively.

We then determined if the DOTA modification of NS changed their blood circulation properties using routinely performed DLS measurement at Nanospectra. Due to safety reasons, we only tested DOTA-NS not radiolabeled NS. Two mice were injected with the DOTA modified particles and another was injected with normal PEGylated particles as a control. The DLS spectrum showed the presence of two distinct peaks. One represented NS and one represented Triton X-100 micelles, and the ratio of the integrated scattering intensity of these two peaks produces a linear model for NS concentration [9]. By graphing the ratios vs. time, we can obtain the circulation information of NS in mouse blood. Figure 2 plots the peak ratios of NS/triton vs. the time after injection and shows the information of NS circulation *in vivo*. All the mice had similar circulation curves, which suggest that the addition of DOTA to NS particles does not affect circulation *in vivo*.

Because the *in vitro* studies showed successful radiolabeling of NS and the *in vivo* study showed that modification of the surface of NS did not change their circulation in mouse blood, we proceeded to test ^{64}Cu-NS and ^{111}In-NS in tumor bearing rats at UTHSC-San Antonio. The rats were imaged at multiple time points post-injection by micro-PET, CT and SPECT. Blood samples were also withdrawn at these time points for radioactive counting. The simulated dual-exponential decay circulation curves were obtained for ^{64}Cu-NS and ^{111}In-NS based on the average percentage of activity remaining in the blood samples from 3 rats at various time points (Figure 3). The data reveals that 61.7% of ^{64}Cu-NS have 0.52 hr half life and 33.8% of ^{64}Cu-NS have 5.29 hr of half life, while 61.53% of ^{111}In-NS have 0.88 hr half life and 35.9% of ^{111}In-NS have 8.07 hr half life in rat blood. The circulation time for both ^{64}Cu-NS and ^{111}In-NS are within the range of normal NS circulation.

As can be seen in Figure 4, PET (A) and SPECT (B) images of the rats showed that both ^{64}Cu and ^{111}In appeared

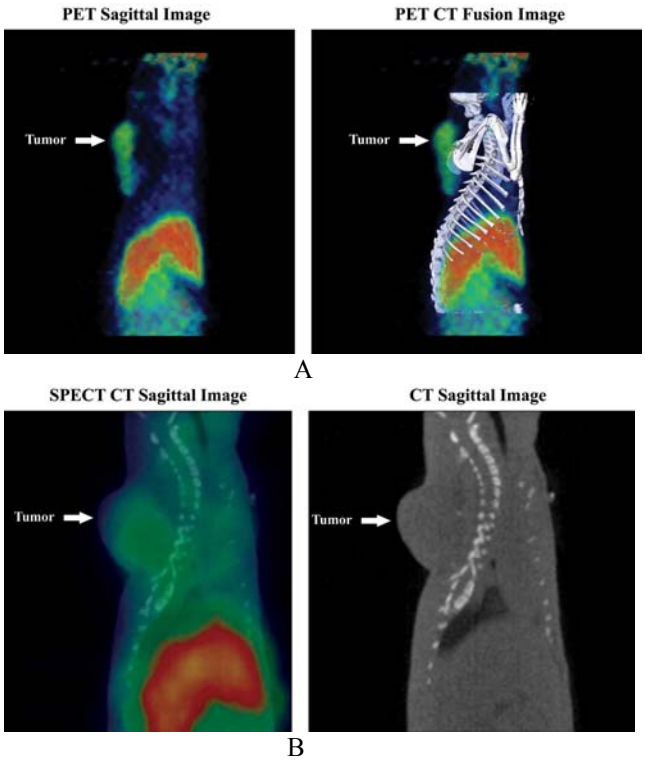

Figure 4: PET/CT (A) and SPECT/CT (B) images of two rats with head and neck tumors at 20 hr post tail-veil injection of ^{64}Cu-NS and ^{111}In-NS.

to be useful for tracking the *in vivo* distribution of nanoshells and both ^{64}Cu-NS and ^{111}In-NS showed obvious uptake of the radiolabeled NS in the tumor. This uptake is likely due to the well described EPR effect. The biodistribution data determined with ^{111}In was very close to that of ^{64}Cu, but image quality was better with the ^{64}Cu. This might be due to the more efficient detection of the ^{64}Cu with the PET ring imaging system than the SPECT camera system. Therefore, PET imaging with ^{64}Cu appears more promising for future nanoshell imaging studies. Imaging provides the possibility not only of quantitative assessment of uptake in the tumor to ensure an adequate uptake for thermal therapy but also can provide localization information to guide the application of infrared thermal therapy.

Recently, small animal and clinical systems have become available that incorporate a CT scanner and a PET camera into the same housing [11]. This permits superimposition of the PET and CT images or SPECT and CT images so that the highly sensitive tracking and quantitation of a PET radiolabeled agent can be localized with the higher anatomic accuracy of CT. The very accurate localization provided by the CT imaging offers the possibility of effective image-guided application of infrared thermal ablation to specific locations of tumor in the body.

This study shows the feasibility of radiolabeling nanoshells for either SPECT or PET imaging using the radiolabeling procedures demonstrated in this article. This technique can be easily adapted for radiolabeling of other types of nanoparticles and radioactive agents. This radiolabeling procedure permits determination of *in vivo* biodistribution and determination of tumor uptake and localization for guidance of laser thermal therapy.

This work was performed under the support of NIST, Advanced Technology Program 70NANB4H3040.

REFERENCES

[1] Oldenberg, S. J., Averitt, R. D., Westcott, S. L. and Halas, N. J. (1998) Nanoengineering of Optical Resonances. Chem. Phys. Lett. **28**, 243-247

[2] O'Neal, D. P., Hirsch, L. R., Halas, N. J., Payne, J. D. and West, J. L. (2004) Photo-thermal tumor ablation in mice using near infrared-absorbing nanoparticles. Cancer Lett. **209**, 171-176

[3] Hirsch, L. R., Stafford, R. J., Bankson, J. A., Sershen, S. R., Rivera, B., Price, R. E., Hazle, J. D., Halas, N. J. and West, J. L. (2003) Nanoshell-mediated near-infrared thermal therapy of tumors under magnetic resonance guidance. Proc Natl Acad Sci U S A. **100**, 13549-13554

[4] Lacerda, L., Soundararajan, A., Singh, R., Pastorin, G., Al-Jamal, K. T., Turton, J., Frederik, P., Herrero, M. A., Li, S., Bao, A., Emfietzoglou, D., Mather, S., Phillips, W. T., Prato, M., Bianco, A., Goins, B. and Kostarelos, K. (2008) Dynamic Imaging of Functionalized Multi-Walled Carbon Nanotube Systemic Circulation and Urinary Excretion. Adv. Mat. **20**, 225-230

[5] Liu, Z., Cai, W., He, L., Nakayama, N., Chen, K., Sun, X., Chen, X. and Dai, H. (2007) In vivo biodistribution and highly efficient tumour targeting of carbon nanotubes in mice. Nature nanotechnology. **2**, 47-52

[6] Cai, W., Shin, D. W., Chen, K., Gheysens, O., Cao, Q., Wang, S. X., Gambhir, S. S. and Chen, X. (2006) Peptide-labeled near-infrared quantum dots for imaging tumor vasculature in living subjects. Nano letters. **6**, 669-676

[7] Wipke, B. T., Wang, Z., Kim, J., McCarthy, T. J. and Allen, P. M. (2002) Dynamic visualization of a joint-specific autoimmune response through positron emission tomography. Nature immunology. **3**, 366-372

[8] Oldenburg, S. J., Jackson, J. B., Westcott, S. L. and Halas, N. J. (1999) Infrared extinction properties of gold nanoshells,. Appl. Phys.Lett. . **111**, 2897

[9] Xie, H., Gill-Sharp, K. L. and O'Neal, D. P. (2007) Quantitative estimation of gold nanoshell concentrations in whole blood using dynamic light scattering. Nanomedicine. **3**, 89-94

[10] Bao, A., Phillips, W. T., Goins, B., McGuff, H. S., Zheng, X., Woolley, F. R., Natarajan, M., Santoyo, C., Miller, F. R. and Otto, R. A. (2006) Setup and characterization of a human head and neck squamous cell carcinoma xenograft model in nude rats. Otolaryngol Head Neck Surg. **135**, 853-857

[11] Rowland, D. J. and Cherry, S. R. (2008) Small-animal preclinical nuclear medicine instrumentation and methodology. Seminars in nuclear medicine. **38**, 209-222